



**HAL**  
open science

## Solidification of ion exchange resins saturated with Na<sup>+</sup> ions: Comparison of matrices based on Portland and blast furnace slag cement

E. Lafond, C. Cau Dit Coumes, S. Gauffinet, D. Chartier, L. Stefan, P. Le Bescop

### ► To cite this version:

E. Lafond, C. Cau Dit Coumes, S. Gauffinet, D. Chartier, L. Stefan, et al.. Solidification of ion exchange resins saturated with Na<sup>+</sup> ions: Comparison of matrices based on Portland and blast furnace slag cement. *Journal of Nuclear Materials*, 2017, 483, pp.121-131. 10.1016/j.jnucmat.2016.11.003 . cea-02380884

**HAL Id: cea-02380884**

**<https://cea.hal.science/cea-02380884>**

Submitted on 26 Nov 2019

**HAL** is a multi-disciplinary open access archive for the deposit and dissemination of scientific research documents, whether they are published or not. The documents may come from teaching and research institutions in France or abroad, or from public or private research centers.

L'archive ouverte pluridisciplinaire **HAL**, est destinée au dépôt et à la diffusion de documents scientifiques de niveau recherche, publiés ou non, émanant des établissements d'enseignement et de recherche français ou étrangers, des laboratoires publics ou privés.

# **Solidification of ion exchange resins saturated with Na<sup>+</sup> ions: comparison of matrices based on Portland and blast furnace slag cement**

E. LAFOND<sup>1</sup>, C. CAU DIT COUMES<sup>1</sup>, S. GAUFFINET<sup>2\*</sup>, D. CHARTIER<sup>1</sup>, L. STEFAN<sup>4</sup>,  
P. LE BESCOP<sup>3</sup>

<sup>1</sup> CEA, DEN, DTCD, SPDE, F-30207 Bagnols-sur-Cèze cedex, France

<sup>2</sup> Laboratoire Interdisciplinaire Carnot de Bourgogne UMR 6303 CNRS-Université de Bourgogne, Dijon, France, 9 Av Alain Savary, BP 47870, 21078 Dijon cedex, France

<sup>3</sup> CEA, DEN, DPC, SECR, F-91192 Gif-sur-Yvette, France

<sup>4</sup> AREVA, Back End Business Group, Dismantling & Services, 1 place Jean Millier 92084 Paris La Défense, France

\*Corresponding author: [sandrine.gauffinet@u-bourgogne.fr](mailto:sandrine.gauffinet@u-bourgogne.fr)

## **Abstract**

Ion exchange resins (IERS) are widely used by the nuclear industry to decontaminate radioactive effluents. After use, they are usually stabilized and solidified by encapsulation in cementitious materials. However, for certain combinations of cement and resins, the solidified waste forms can exhibit strong expansion, possibly leading to cracking of the matrix.

In this work, the behaviour of cationic resins in the  $\text{Na}^+$  form is investigated in Portland cement (CEM I) or blast furnace slag cement (CEM III/C) pastes at early age in order to have a better understanding of the swelling process. The results show that during the hydration of the CEM I paste, the resins exhibit a transient expansion of small magnitude due to the decrease in the osmotic pressure of the pore solution. This expansion, also observed with  $\text{C}_3\text{S}$  pastes containing similar IERS, occurs just after setting and is sufficient to damage the material which is poorly consolidated. In the CEM III/C paste, expansion of the resins occurs before the end of setting and only induces limited stress in the matrix which is still plastic.

**Keywords** : ion exchange resins, swelling, hydration, Portland cement, blast furnace slag cement

## 1 **1. Introduction**

2 Ion exchange resins (IERS) are commonly used by the nuclear industry in the decontamination  
3 process of radioactive effluents. The spent resins become a low-level or intermediate-level radioactive  
4 waste and have to be stabilized and solidified, i.e. placed under a solid, stable, monolithic and  
5 confining form, before being sent to disposal. Calcium silicate cements offer many advantages for  
6 resins encapsulation: easy supply, simple process, good mechanical strength, compatibility with  
7 aqueous wastes, good self-shielding, and high alkalinity which allows many radionuclides to be  
8 precipitated and thus confined. However, for certain combinations of cement and resins, the solidified  
9 waste forms can exhibit strong dimensional variation, possibly leading to cracking of the matrix.

10 Several specificities of IERS have to be taken into account to design a robust cement-based matrix,  
11 such as low intrinsic mechanical strength and possible ionic exchanges with the pore solution [1, 2]. It  
12 is also well known that in aqueous medium, the volume of IERS beads strongly depends on the  
13 composition of the solution. Expansion or shrinkage can be caused by ionic exchanges and/or  
14 variations in osmotic pressure. These volume changes can also occur in a cementitious matrix, the  
15 pore solution chemistry of which evolves with ongoing hydration and, under severe conditions, they  
16 can induce cracking of the matrix [3-5]. Knowledge about the chemical evolution of IERS in a  
17 cementitious environment is limited. For example, it is often mentioned in the literature that the  
18 encapsulation of IERS with Portland cement (CEM I) leads to strong expansion during the early stages  
19 of cement hydration, whereas no swelling is observed when Portland cement is blended with high  
20 amounts of blast furnace slag [6,7]. However, the reasons for these different behaviours are not  
21 understood.

22 To simplify the system under investigation, Portland cement was replaced in a previous study by its  
23 main component, tricalcium silicate [8]. The  $C_3S$ -waste form also exhibited a strong expansion and  
24 two main stages were observed during hydration at early age. In the first one, due to ionic exchange  
25 (fixation of calcium, release of sodium), the resins shrank. Then, in a second stage, as hydration  
26 accelerated, the sodium concentration in the pore solution rapidly decreased due to the precipitation of  
27 sodium-bearing C-S-H, whereas the resins continued to fix calcium ions. Swelling of the resins  
28 occurred during the second stage, and resulted from the decrease in the osmotic pressure of the pore

29 solution due to the consumption of sodium ions. Despite its small magnitude, swelling seemed to be  
30 enough to deteriorate the hardened matrix during the second stage, just after setting, while the degree  
31 of hydration was still low and the matrix poorly consolidated.

32 To provide deeper understanding of real systems, this work aims at comparing the hydration of  
33 Portland cement and blast furnace slag cement (CEM III/C) pastes with cationic resins initially in the  
34  $\text{Na}^+$  form. The objective is to explain why cements containing high amounts of blast furnace slag are  
35 more appropriate than Portland cement to solidify and stabilize this waste.

36

## 37 **2. Experimental**

38

### 39 **2.1 Materials**

40

41 The two cements used in this study were referred as CEM III/C (32.5 N from Calcia Rombas) and  
42 CEM I (52.5 N from Calcia Couvrot). According to European standard EN 197-1:2000, CEM I  
43 comprises 95-100% Portland Cement clinker whereas CEM III/C corresponds to a Blast Furnace  
44 Cement consisting of 5-19% Portland cement clinker and 81-95% blast furnace slag. The  
45 compositions of the cements and clinker are reported in Tables 1 and 2. The two cements comprised  
46 the same Portland clinker, but in different amounts.

47 IERs were supplied by Rohm&Haas under the trade name Amberlite IR120H in the physical form of  
48 spherical beads or ground grains. The IER beads had a diameter comprised between 620 and 830  $\mu\text{m}$ ,  
49 and the ground IERs had a particle size ranging from 0.4  $\mu\text{m}$  to 300  $\mu\text{m}$  ( $d_{10} = 15 \mu\text{m}$ ,  $d_{50} = 65 \mu\text{m}$ ,  $d_{90}$   
50  $= 155 \mu\text{m}$ ). The exchange sites of the resins, shipped in the  $\text{H}^+$  form, were saturated with  $\text{Na}^+$  ions by  
51 percolating a solution of sodium hydroxide. The pH of the eluted solution was continuously  
52 monitored, and the percolation was stopped as soon as the pH exceeded 7. The resins were then rinsed  
53 with water to eliminate the excess of base and to recover a neutral pH. Finally, the suspension of  
54 water and resins was filtered under humid atmosphere and slight vacuum on a Buchner funnel to  
55 remove the free intergranular water (water between the resin grains). The dry extract of the wet resins  
56 was measured by gentle heating at 55°C (to avoid any damage of the functional groups) until constant

57 weight. Values of  $54.3 \pm 0.2 \%$  and  $45.3 \pm 0.2 \%$ . were achieved for beads and ground grains  
58 respectively. This difference was explained by the fact that ground resins developed a larger surface  
59 area than bead resins. The volume of water adsorbed onto the surface of resin was thus more  
60 important. The wet resins were kept in tightly closed containers. The resins were used in their ground  
61 form, except for SEM observations where beads were preferred.

62

## 63 **2.2 Preparation of samples**

64

65 Experiments were conducted on pure cement pastes, consisting of CEM III/C or CEM I cement and  
66 water, as well as on cement pastes mixed with IERs.

67 To prepare pure cement pastes, CEM III/C or CEM I cements were introduced in a standardized  
68 laboratory mixer (European Standard EN 196-1) with water, mixed at low speed for 30 s and at high  
69 speed for 3 min. The water-to-cement ratio was fixed to 0.55, which corresponded to the effective  
70 water-to-cement ratio of the pastes with IERs, calculated by correcting the total amount of water from  
71 that retained in the IERs to solvate the ionic groups. This latter was assessed by measuring their dry  
72 extract after the saturation step with  $\text{Na}^+$  ions, as previously explained in section 2.1. The pure cement  
73 pastes exhibited transient bleeding which disappeared after setting.

74 Mixing of cement/IERs systems was performed in two steps: IERs and water were first stirred during  
75 30 s at low speed in a standardized laboratory mixer. Then, cement (CEM I or CEM III/C) was  
76 introduced in the mixer, mixed at low speed for 30 s and at high speed for 3 min. Samples contained  
77 11 wt. % of dry resins, and a total water-to-cement ratio of 0.8. The high water content enabled to get  
78 workable grouts and ensured that the system remained saturated, at least at early age.

79 The fresh grout samples were cast into hermetically sealed 50 mL-polypropylene containers and  
80 stored in a climatic chamber at  $20^\circ\text{C}$  with 95% relative humidity until characterization.

81

## 82 **2.3 Characterization of hydration**

83

84 The Vicat setting time was measured using an automatic Vicat needle apparatus according to EN 196-  
85 3 standard. In addition, to point out the different stages of hydration, calorimetric measurements were  
86 carried out using isothermal microcalorimetry at 25°C (SETARAM, C80 type). Hydration was also  
87 stopped after fixed periods of time (from 1 hour to 10 days) by successively immersing the crushed  
88 pastes into isopropanol and drying them in a controlled humidity chamber (with 20% relative  
89 humidity at  $22 \pm 2^\circ\text{C}$ ). After grinding to a particle size below 80  $\mu\text{m}$ , the mineralogy of the cement  
90 pastes was characterized by X-ray diffraction (Siemens D8, copper anode,  $\lambda_{\text{CuK}\alpha 1}=1.54056 \text{ \AA}$ ). A semi-  
91 quantitative analysis was performed to assess the evolution of the amounts of reactants and products  
92 with time using EVA analysis software (© 2005 Bruker AXS). The method consisted in introducing an  
93 internal standard (10 wt% silicon, correction made to take into account the increasing amount of  
94 bound water with ongoing hydration) into the sample to be analysed by XRD, and then in calculating  
95 the ratio between the area of the most intense diffraction peak of the phase to quantify and that of  
96 silicon. The microstructure evolution was observed by Scanning Electron Microscopy (FEI Inspect  
97 S50, high vacuum mode, acceleration voltage of 15 kV, current intensity of 50 nA) on sample  
98 fractures and polished section at different ages. The Na/S, Ca/S, Na/Si and Ca/Si ratios in the hydrates  
99 and IER grains were determined by X-ray microanalysis on polished cross sections (high vacuum  
100 mode, Bruker SDD detector calibrated on jadeite,  $\text{FeS}_2$  and wollastonite).

101 The pore solutions of cement pastes were extracted using pressure (34 MPa) from 1 hour to 10 days.  
102 The  $\text{Na}^+$ ,  $\text{K}^+$ ,  $\text{Ca}^{2+}$ , and  $\text{SO}_4^{2-}$  concentrations were determined using ionic chromatography (Dionex  
103 DX500 equipped with IonPac CS12A analytical column and IonPac CG12A guard column). The  
104 analytical error was  $\pm 5\%$ .

105

## 106 **2.4 Characterisation of volumetric change**

107

108 The shrinkage cone method was used to follow the apparent volumetric change of cement-waste  
109 forms with ongoing hydration. It was initially developed by the German Cement Works Association  
110 for measuring the autogenous shrinkage of concrete [9]. The setup (from Schleibinger Geräte)  
111 consisted of a laser vertically pointed at the surface of a cone-shaped sample in a cylindrical jar

112 connected to a thermostatic bath at 25°C. The sample was poured into the jar and slightly vibrated.  
113 The surface of the sample was covered with a plastic sheet equipped with a reflector to avoid  
114 desiccation. The jar was then placed underneath the laser, and the distance variation between the  
115 reflector and the laser was recorded every 10 minutes. The measurement range was 5 mm, with a  
116 resolution of 0.1 μm. The cone geometry ensured that the change in height corresponded to the linear  
117 length change of the material as long as it was fluid and also after solidification since deformation was  
118 considered as uniform.

119 Based on the work of Matsuda [4], an oedometric cell was developed to measure the swelling pressure  
120 induced by cemented resins under constrained environment. 20 g of paste samples were introduced in  
121 a cylindrical cell containing a metallic fritted disc at the bottom (Figure 1). A second fritted disc was  
122 placed on the upper surface sample and the cell was tightly closed with a piston connected to force  
123 sensor. An initial pressure of 0.1 MPa was applied. Measuring the increase in the axial stress enabled  
124 to follow the swelling pressure of samples with time.

125

### 126 **3. Results**

127

#### 128 **3.1 Volumetric change with ongoing hydration**

129

130 Figure 2 shows the evolution of the swelling pressure of cement-IERs forms under constant strain. As  
131 expected, the pressure increased only for the CEM I sample. Tests with the shrinkage cone showed  
132 that, under unconfined conditions, this sample also exhibited a strong apparent volume increase which  
133 began 8 h after mixing and exceeded 7% after 220 h.

134

#### 135 **3.2 Characterization of hydration**

136

137 The Vicat setting time of the CEM I and CEM III/C cement pastes was measured with or without  
138 IERs in Na<sup>+</sup> form. The results are presented in Table 3. The presence of IERs tended to accelerate the  
139 setting of both cements. Setting started 30 min earlier, and ended from 1 h (CEM III/C) to 2.75 h

140 (CEM I) earlier than in the corresponding pure cement pastes. These results were consistent with the  
141 heat flow measurements (Figure 3), showing a slight acceleration of the heat production in the  
142 samples containing resins. The setting of the CEM III/C samples remained however much slower than  
143 that of the CEM I samples because of the low reactivity of blast furnace slag as indicated by the  
144 reduced heat production (Figure 3).

145

### 146 **3.3 Pore solution evolution**

147

148 Figures 4 and 5 show the evolution of the pore solution composition and corresponding osmotic  
149 pressure (from 1 h to 10 d) for CEM I and CEM III/C paste samples with and without resins.

150 The osmotic pressure of the pore solution was calculated using Van't Hoff equation (1).

$$151 \quad \pi = \Phi RT \sum_i c_i \quad (1)$$

152 where  $\pi$  is the osmotic pressure of the solution (Pa),  $\phi$  the osmotic coefficient, R the constant of ideal  
153 gases (8.314 J.mol<sup>-1</sup>.K<sup>-1</sup>), T the temperature (K) and  $c_i$  the concentration of ion  $i$  in solution (mol.L<sup>-1</sup>).

154 The osmotic coefficient is a corrective factor taking into account the non-ideal behavior of the  
155 solution. It was calculated using PhreeQC [10] and Pitzer's thermodynamic database [11].

156 In both materials, the sodium concentration rapidly increased during the first 8 h and reached a  
157 maximum which corresponded to about 1/3 of the sodium initially fixed by the resins (35% for CEM I  
158 sample, 30% for CEM III/C sample). The potassium concentration was much lower than in the pure  
159 cement pastes. It was also the case for the calcium concentration, but to a lesser extent.

160 These results showed a partial exchange of Na<sup>+</sup> ions from the resins with Ca<sup>2+</sup> and K<sup>+</sup> ions released by  
161 the dissolution of the cement anhydrous phases. In the same time, the sulphate concentration  
162 increased due to the dissolution of gypsum. As a result, the osmotic pressure of the pore solution also  
163 increased. From previous studies devoted to the volume change of IERs depending on their chemical  
164 environment [8, 12], it could be concluded that the 2Na<sup>+</sup> ↔ Ca<sup>2+</sup> and Na<sup>+</sup> ↔ K<sup>+</sup> exchanges as well as  
165 the increase in the osmotic pressure should cause a shrinkage of the IERs during this period. K<sup>+</sup> ions  
166 have indeed a smaller solvated ionic radius (~3.2 Å) than Na<sup>+</sup> ions (~4.0 Å) [13]. As for calcium, its

167 solvation ionic radius is close to that of  $\text{Na}^+$ , but since it is a divalent cation, its concentration in the  
168 resins is divided by a factor 2. Besides, when the osmotic pressure of the solution external to the  
169 resins increases, water tends to get out of the resins to reduce the external concentration and  
170 equilibrate the chemical potentials between the external and internal solutions.

171

172 Then, a second stage occurred. Sulphate ions were depleted from the interstitial solution due to the  
173 precipitation of ettringite (the exhaustion of gypsum was also observed by XRD at the same time,  
174 Figures 6 and 7). The sodium concentration in solution also decreased. As a consequence, the osmotic  
175 pressure of the external solution diminished, which produced a swelling of the IERs [8, 12]. Its  
176 magnitude was assessed using previously established calibration curves plotting the volume of  $\text{Na}^+$ -,  
177  $\text{K}^+$ -, and  $\text{Ca}^{2+}$ -IER beads versus the osmotic pressure of the external solution [8, 12, 14]. It was close  
178 to 0.1 % for the IERs-CEM I sample, and 0.19 % for IERs-CEM III/C sample.

179

### 180 **3.4 IERs analysis**

181

182 X-ray microanalyses were performed on polished cross-sections of pastes with IER beads after 2 and  
183 24 hours of hydration. For each hydration time, 10 IER grains were selected and more than 10  
184 analyses were performed on each grain. The average Na/S, Ca/S and K/S ratios measured on samples  
185 aged of 2 h and 24 h are given in Table 4. The results confirmed the fixation of  $\text{Ca}^{2+}$  and  $\text{K}^+$  ions by  
186 the resins during the early stages of hydration. The Na/S ratio continuously diminished with time.  
187 Thus, the decrease in the sodium concentration observed in the pore solution after 8 h (CEM I) or 3 h  
188 (CEM III/C) was not due to re-fixation of  $\text{Na}^+$  ions on the resins, with simultaneous release of  $\text{K}^+$  or  
189  $\text{Ca}^{2+}$  ions in solution.

190

### 191 **3.5 Mineralogy evolution**

192

193 The mineralogy of the different investigated systems was characterized by XRD and SEM. The CEM  
194 I-based materials comprised C-S-H, portlandite, ettringite as well as residual anhydrous cement

195 phases (Figure 6). In the CEM III/C-based materials, the same hydrates were detected with the  
196 exception of portlandite (Figure 7). For a given type of cement, the resins did not change the nature of  
197 the precipitated hydrates, but only influenced their rate of formation (Figure 8).

198 In both cement-IERs systems, X-ray microanalysis performed on polished cross-sections of 24h-old  
199 samples showed that C-S-H sometimes comprised significant amounts of sodium. This sodium-  
200 bearing C-S-H was very heterogeneously distributed in the matrix, with an average Na/Si ratio close  
201 to 0.2 after 24 h. Its precipitation could explain the second decrease in the sodium concentration of the  
202 pore solution. The formation of both C-S-H and C-N-S-H has also been reported when resins in the  
203 Na<sup>+</sup> form are encapsulated in a C<sub>3</sub>S paste [8], or during the hydration of blast-furnace slag activated  
204 by a concentrated NaOH solution [15].

205 SEM observations of fractures also confirmed the precipitation of portlandite in the IERs-CEM I  
206 sample, as big crystals of a few 100 μm (Figure 9-a) at the interface between IER grains and paste.  
207 This localized precipitation seemed consistent with the results presented in sections 3.3 and 3.4. The  
208 shrinkage of the resins in the first stage of hydration would create voids at the resin/paste interface  
209 where portlandite could precipitate. Besides, the strong affinity of the resins for calcium ions would  
210 induce a calcium flux from the paste to the resins, possibly leading to a local supersaturation with  
211 respect to portlandite near the resin beads. By contrast, in the IERs-CEM III/C samples, no portlandite  
212 precipitation was observed (Figure 9-b).

213

#### 214 **4. On the swelling of IERs-CEM I samples**

215

216 The CEM I- and CEM III/C-based materials differed by their consolidation rate. When resins were  
217 encapsulated in the CEM III/C matrix, expansion occurred between the beginning and the end of Vicat  
218 setting, when the material was still plastic. The CEM I cement exhibited a higher rate of hydration,  
219 and swelling of the IERs occurred just a few hours after the Vicat end of setting, in a hardened matrix,  
220 but with:

- 221 - (i) low mechanical strength. As a fact, when calcium ions are progressively replaced by  
222 monovalent cations such as sodium ions, the cohesion decreases, and repulsion between C-S-H

223 particles can even be observed if the negative surface charge density is balanced by monovalent  
224 cations only [16, 17]. Precipitation of C-N-S-H in the pastes with Na<sup>+</sup>-IERs could thus contribute  
225 to reduce the strength of the matrix.

226 - (ii) heterogeneous microstructure. Highly porous transition zones were observed between IER  
227 grains and the cement paste with precipitation of large crystals of portlandite.

228 Despite its small magnitude, the swelling of IERs due to the decrease in the osmotic pressure of the  
229 pore solution could be sufficient to induce cracking of the poorly consolidated matrix.

230 To check this assumption, complementary experiments were carried out on IERs-CEM I samples by  
231 retarding the setting without notable change in the chemical evolution. To this end, the fresh grout was  
232 divided in two samples which were cured at two different temperatures, 5 and 20 °C. The damage of  
233 the cement-resin forms was assessed qualitatively by visual observation (Table 5, Figure 10).  
234 Extractions of solutions were performed at 1 h, 5 h, 7 h, 24 h, 48 h and 7 d. The Vicat setting time was  
235 also measured at both temperatures. Results are reported in Figure 11.

236 The ionic concentrations showed very similar evolutions with time at both temperatures; the decrease  
237 in temperature thus did not affect significantly the chemical evolution of the systems at early age,  
238 showing that ionic exchanges on the resin grains, which are very fast, played a key role during this  
239 period. Decreasing the temperature however delayed the beginning and end of setting by 8.5 h. As  
240 observed before, at 20 °C, the end of setting occurred when the sodium concentration was at its  
241 maximum, corresponding to resins under their most contracted form. The slight expansion of the  
242 resins caused by the decrease in the osmotic pressure of the interstitial solution (exhibiting the same  
243 trend as the sodium concentration) took place just after setting, leading to cracking and disintegration  
244 of the sample. At 5°C, setting occurred once the resins had started to swell, and the damages were  
245 much less important. The consolidation rate thus seemed to be a key parameter to explain expansion  
246 and damage of IERs-CEM I materials.

247

## 248 **5. Conclusions**

249

250 The results show that during the hydration of CEM I and CEM III/C cement pastes, the resins exhibit  
251 a transient expansion of small magnitude due to the decrease in the osmotic pressure of the interstitial  
252 solution. This expansion occurs just after setting for IERs-CEM I forms. It is sufficient to damage the  
253 material which is poorly consolidated with heterogeneous microstructure. Expansion of the IERs-  
254 CEM III/C forms is not observed because CEM III/C cement exhibits a slower rate of hydration than  
255 CEM I cement. Transient expansion of the resins takes place before the end of setting and only  
256 induces limited stress in the material which is still plastic.

257

## 258 REFERENCES

- 259 [1] V. Morin, S. Garrault, F. Begarin, I. Dubois-Brugger, The influence of an ion-exchange resin  
260 on the kinetics of hydration of tricalcium silicate, *Cem. Concr. Res.* 40 (2010) 1459-1464.
- 261 [2] Q. Sun, J. Li, J. Wang, Solidification of borate radioactive resins using sulfoaluminate cement  
262 blended with zeolite, *Nucl. Eng. Design* 241 (2011) 5308-5315.
- 263 [3] P. Soo, L.W. Milian, The impact of LWR decontamination on solidification, waste disposal and  
264 associated occupational exposure. Effect of composition on the strength, swelling and water-  
265 immersion properties of cement-solidified ion-exchange resin wastes, Brookhaven National  
266 Laboratory, NUREG/CR-3444 (1991).
- 267 [4] M. Matsuda, M. Kikuchi, T. Takashi, Conditioning of spent ion exchange resin using high  
268 performance cement, *Proc. Waste Management*, Tucson, Arizona (1993).
- 269 [5] G.W. Veazey, R.L. Ames, Cement waste-form development for ion exchange resins at the  
270 Rocky Flats plant, Los Alamos National Laboratory, LA-13226-MS UC-721 (1997).
- 271 [6] M. Matsuda, T. Nishi, K. Chino, M. Kikuchi, Solidification of Spent Ion-Exchange Resin Using  
272 New Cementitious Material .1. Swelling Pressure of Ion-Exchange Resin, *J. Nucl. Sci.*  
273 *Techn.*(1992) 883-889.
- 274 [7] V.N Epimakhov, M.S Oleinik, Inclusion of radioactive ion-exchange resins in inorganic  
275 binders, *Atomic Energy*, 99 (2005) 607-611.

- 276 [8] E. Lafond, C. Cau Dit Coumes, S. Gauffinet, D. Chartier, P. Le Bescop, L. Stefan, A. Nonat,  
277 Investigation of the swelling behaviour of cationic exchange resins saturated with Na<sup>+</sup> ions in  
278 C<sub>3</sub>S paste, *Cem. Conc. Res.* 69 (2015) 61-71.
- 279 [9] S. Eppers, C. Müller, The shrinkage cone method for measuring the autogenous shrinkage: an  
280 alternative to the corrugated tube method, *Proc. International RILEM conference on the use of*  
281 *superabsorbent polymers and other new additives in concrete*, Lyngby, Denmark (2010) 67-76.
- 282 [10] D.L. Parkurst, D.C. Thorstenson, L.N. Plummer, PHREEQC, A Computer Program for  
283 Geochemical Calculations: U.S. Geological Survey Water-Resources Investigations, Report 80–  
284 96, 195 (1980) (revised and reprinted August 1990).
- 285 [11] L.N. Plummer, D.L. Parkhurst, G.W. Flemming, S.A. Dunkle, A computer program  
286 incorporating Pitzer's equations for calculation of geochemical reactions in brines, US  
287 Geological Survey, Water-Resources Investigation Report 88 4153 (1988).
- 288 [12] E. Lafond, Etude chimique et dimensionnelle de résines échangeuses d'ions cationiques en  
289 milieu cimentaire, PhD thesis, Université de Bourgogne, France (2013).
- 290 [13] W. Rieman, H.F. Walton, Ion exchange in analytical chemistry, Pergamon Press, Oxford, Great  
291 Britain, (1970) 24-27.
- 292 [14] C. Cau Dit Coumes, E. Lafond, S. Gauffinet, D. Chartier, P. Le Bescop, L. Stefan, A. Nonat, On  
293 the swelling behavior of cationic exchange resins saturated with Na<sup>+</sup> ions in a C<sub>3</sub>S or Portland  
294 cement paste, *Proc. NUWCEM 2014*, 3-6 juin, Avignon, France (2014).
- 295 [15] M. Ben Haha, G. Le Saout, F. Winnefeld, B. Lothenbach, Influence of activator type on  
296 hydration kinetics, hydrate assemblage and microstructural development of alkali activated  
297 blast furnace slags, *Cem. Concr. Res.* 41 (2011) 301-310.
- 298 [16] S. Lesko, Mesure des forces interparticulaires par microscopie à force atomique. Application à  
299 la cohésion des ciments, PhD thesis, Université de Bourgogne, France (2005).
- 300 [17] C. Labbez, B. Jonsson, I. Pochard, A. Nonat, B. Cabane, Surface charge density and  
301 electrokinetic potential of highly charged minerals: experimental and Monte Carlo simulations  
302 on calcium silicate hydrate, *J. Chem. Phys. B.* 110 (2006) 9219-9230.
- 303



308 Table 2: Composition of CEM III/C cement (oxide composition determined by X ray fluorescence,  
 309 phase composition determined by Rietveld analysis).

	CaO	SiO <sub>2</sub>	Al <sub>2</sub> O <sub>3</sub>	Fe <sub>2</sub> O <sub>3</sub>	SO <sub>3</sub>	K <sub>2</sub> O	Na <sub>2</sub> O	MgO	MnO	TiO <sub>2</sub>	P <sub>2</sub> O <sub>5</sub>
<b>Chemical</b>											
<b>composition of</b>	45.1	32.0	10.3	0.8	2.9	0.55	0.18	6.1	0.4	0.5	0.1
<b>cement (wt. %)</b>											
<b>Phase</b>		C <sub>3</sub> S: 66							Blast furnace slag: 80.5		
<b>composition of</b>		C <sub>2</sub> S: 13			<b>Cement composition</b>				Clinker: 14.2		
<b>clinker (wt.%)</b>		C <sub>3</sub> A: 11			<b>(wt.%)</b>				Anhydrite: <b>5.2</b>		
		C <sub>4</sub> AF: 7									

310

311

312 Table 3: Vicat setting times of CEM I and CEM III/C cement pastes with and without IERs ( $\pm 0.3$  h).

<b>Sample</b>	<b>Beginning of setting (h)</b>	<b>End of setting (h)</b>
<b>CEM I</b>	4.0	11.3
<b>CEM I + IERs</b>	3.5	8.5
<b>CEM III/C</b>	6.5	31.0
<b>CEM III/C + IERs</b>	6.0	30.0

313

314

315 Table 4: Na/S, Ca/S and K/S molar ratios of resin beads encapsulated in a CEM I or CEM III/C  
 316 cement paste.

Type of cement	Age of sample (h)	Na/S		Ca/S		K/S	
		Average	Standard deviation	Average	Standard deviation	Average	Standard deviation
<b>CEM I</b>	2	0.86	0.06	0.03	0.03	0.14	0.02
	24	0.78	0.05	0.07	0.02	0.19	0.01
<b>CEM III/C</b>	2	0.85	0.07	0.08	0.06	0.03	0.01
	24	0.79	0.07	0.10	0.06	0.04	0.01

317

318

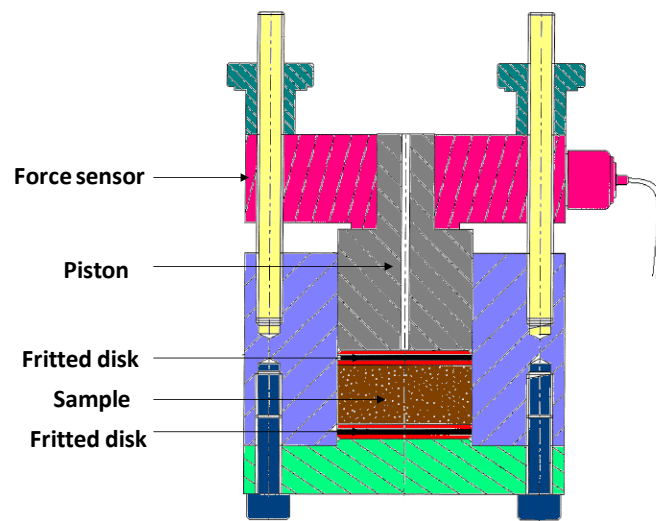
319 Table 5: Visual observations of IERs-CEM I and IERs-CEM III/C samples cured at 25°C and 5°C.

Hydration time	25°C	5°C
<b>3 days</b>	Apparition of the first cracks	No cracks
<b>6 days</b>	Destruction of the container	Slight cracks on the container
<b>10 days</b>	Destruction of the sample	Slight cracks on the container

320

321

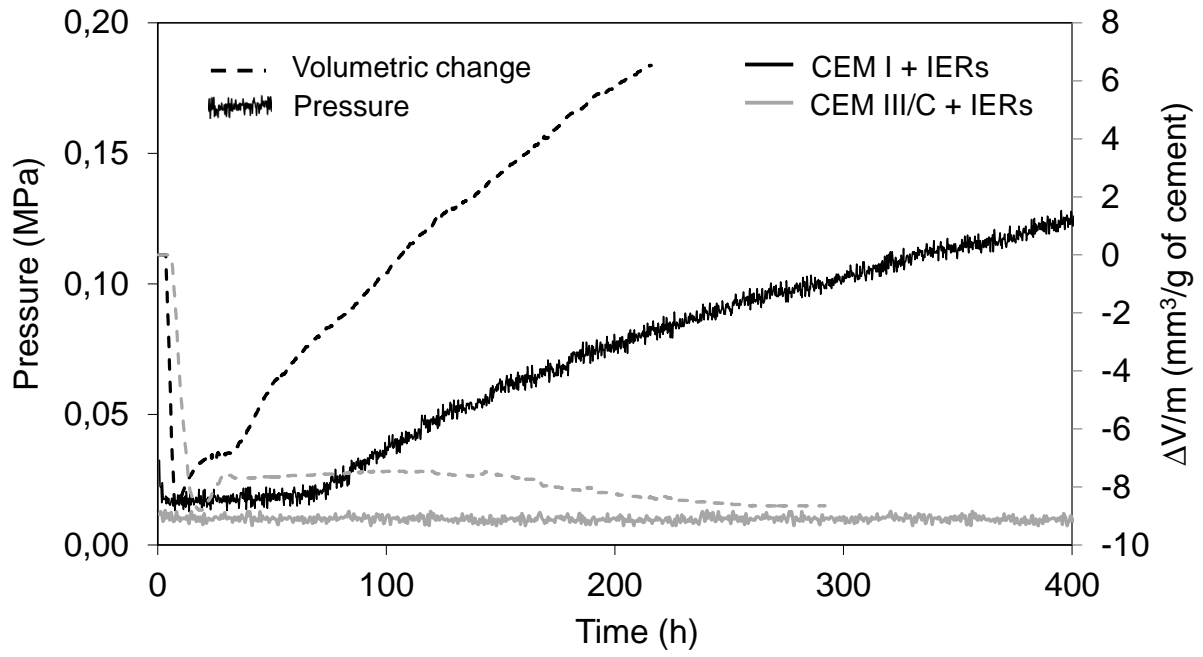
322 Figure 1: Experimental device to measure swelling pressure under constrained environment.



323

324

325 Figure 2: Evolution with time of the pressure induced by IERs-CEM I and IERs-CEM III/C samples  
326 under confined environment; comparison with their volumetric change under unconfined  
327 environment.

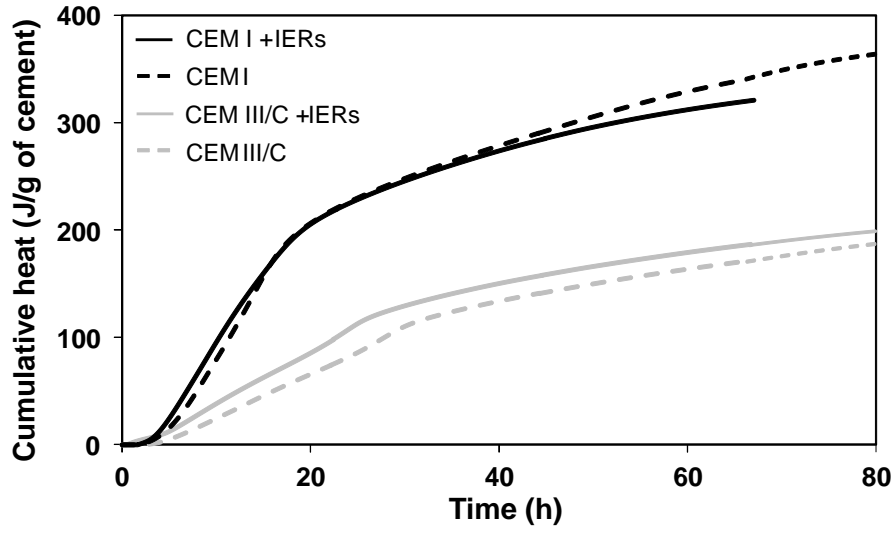


328  
329  
330

331

332 Figure 3: Cumulative heat flow versus time for CEM I and CEM III/C cement pastes with and without

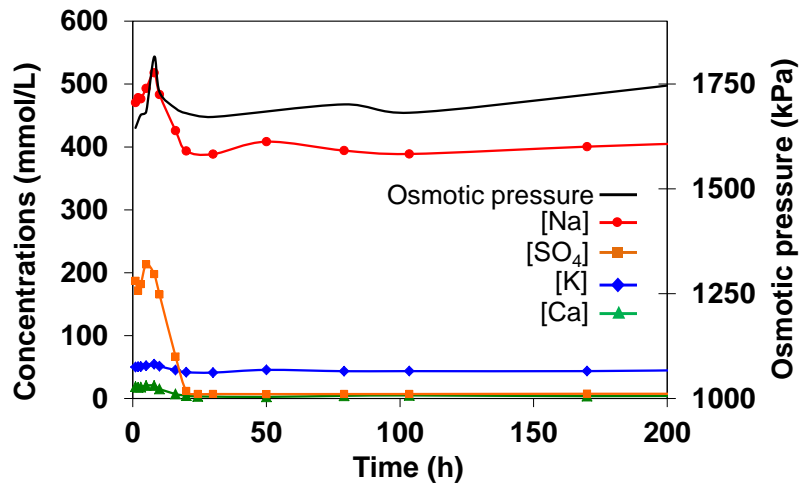
333 IERs.



334

335

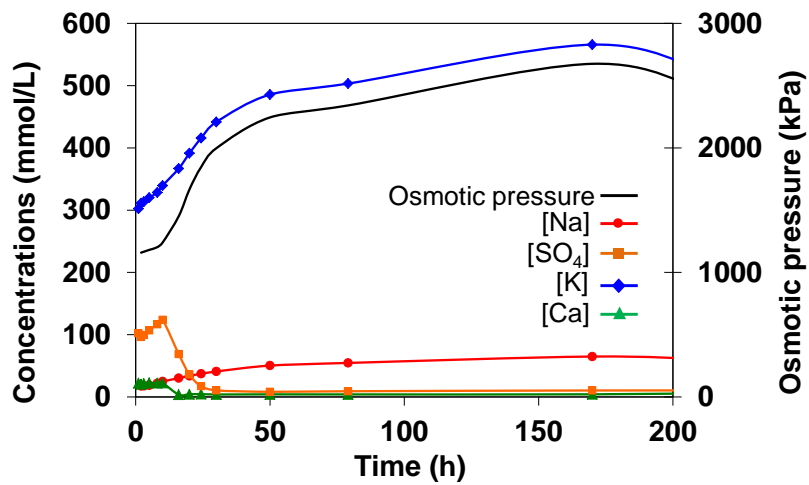
336 Figure 4: Evolution of the composition ( $\text{Na}^+$ ,  $\text{K}^+$ ,  $\text{Ca}^{2+}$ ,  $\text{SO}_4^{2-}$ ) and osmotic pressure of the interstitial  
337 solution of CEM I cement paste samples with (a) and without resins (b).



338

339

(a)



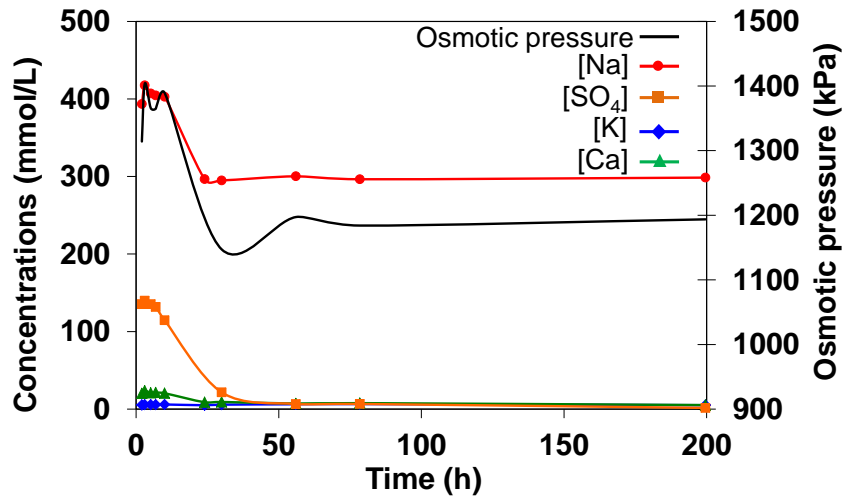
340

341

342

(b)

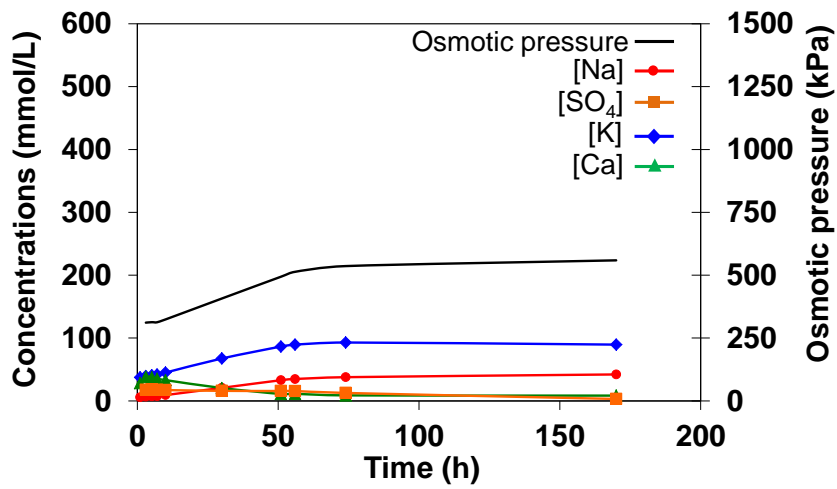
343 Figure 5: Evolution of the composition ( $\text{Na}^+$ ,  $\text{K}^+$ ,  $\text{Ca}^{2+}$ ,  $\text{SO}_4^{2-}$ ) and osmotic pressure of the interstitial  
 344 solution of CEM III/C cement pastes with (a) or without IERs (b).



345

346

(a)



347

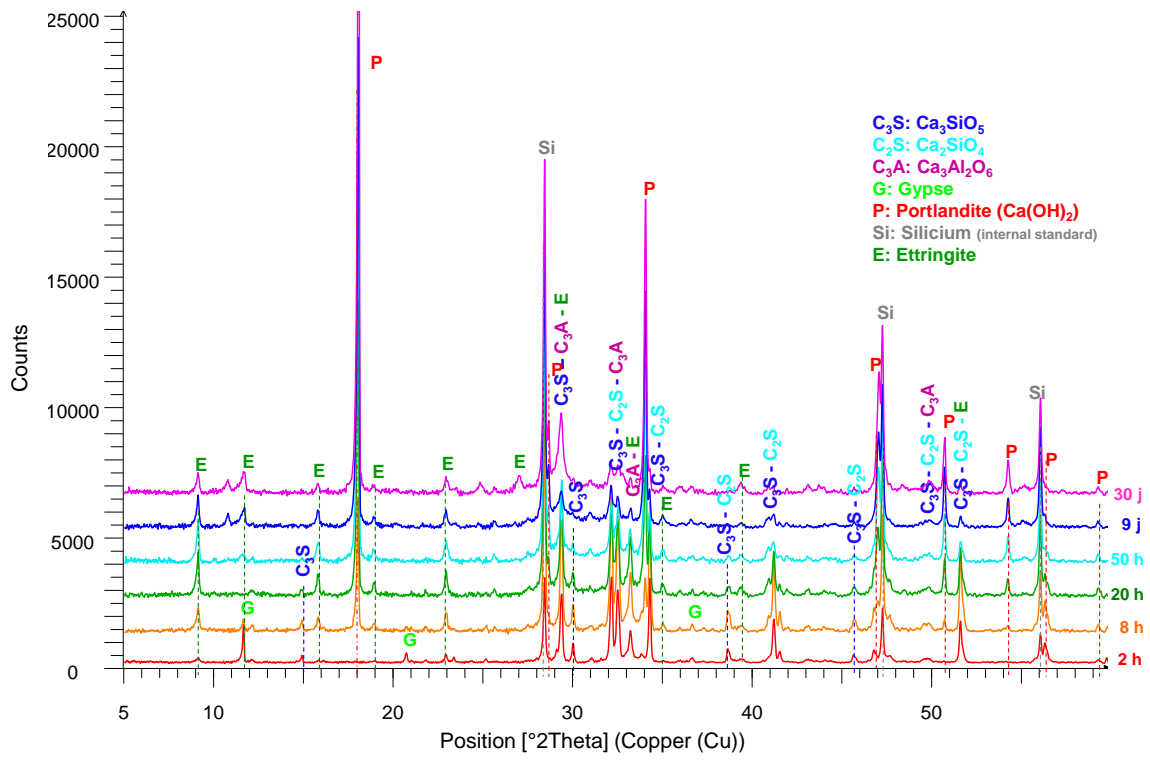
348

349

350

(b)

351 Figure 6: X-ray diffraction patterns of IERs-CEM I samples.

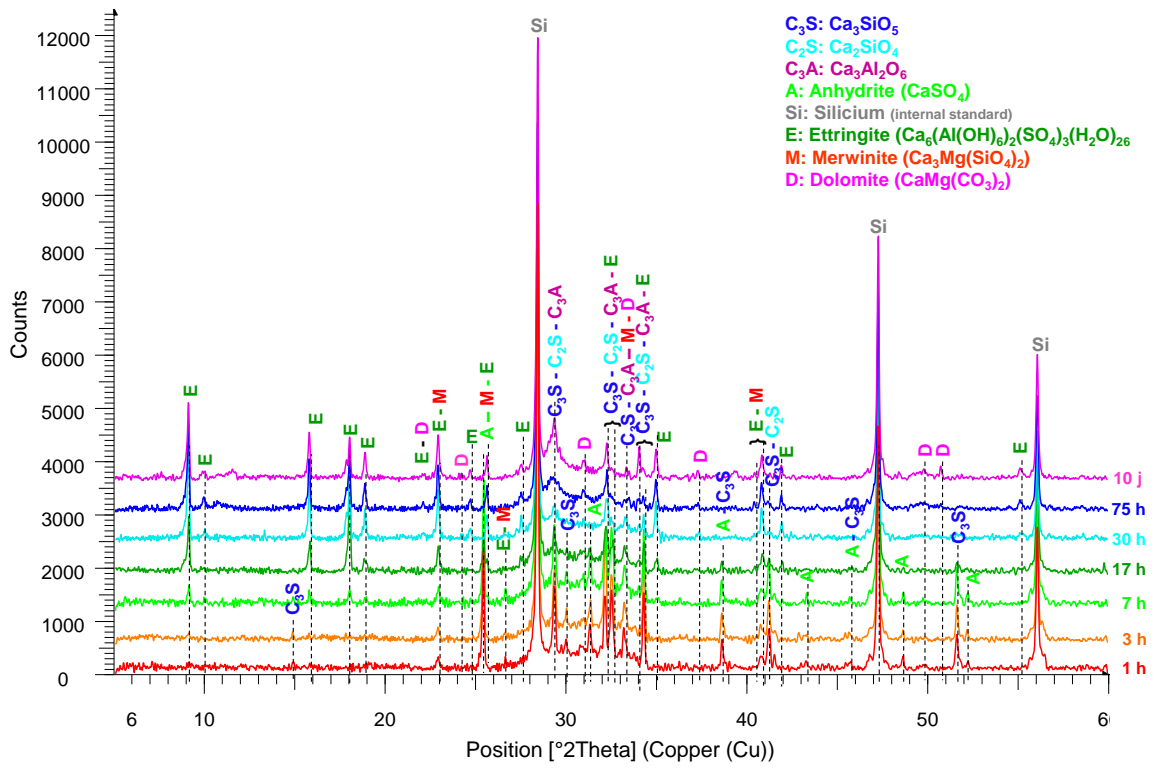


352

353

354

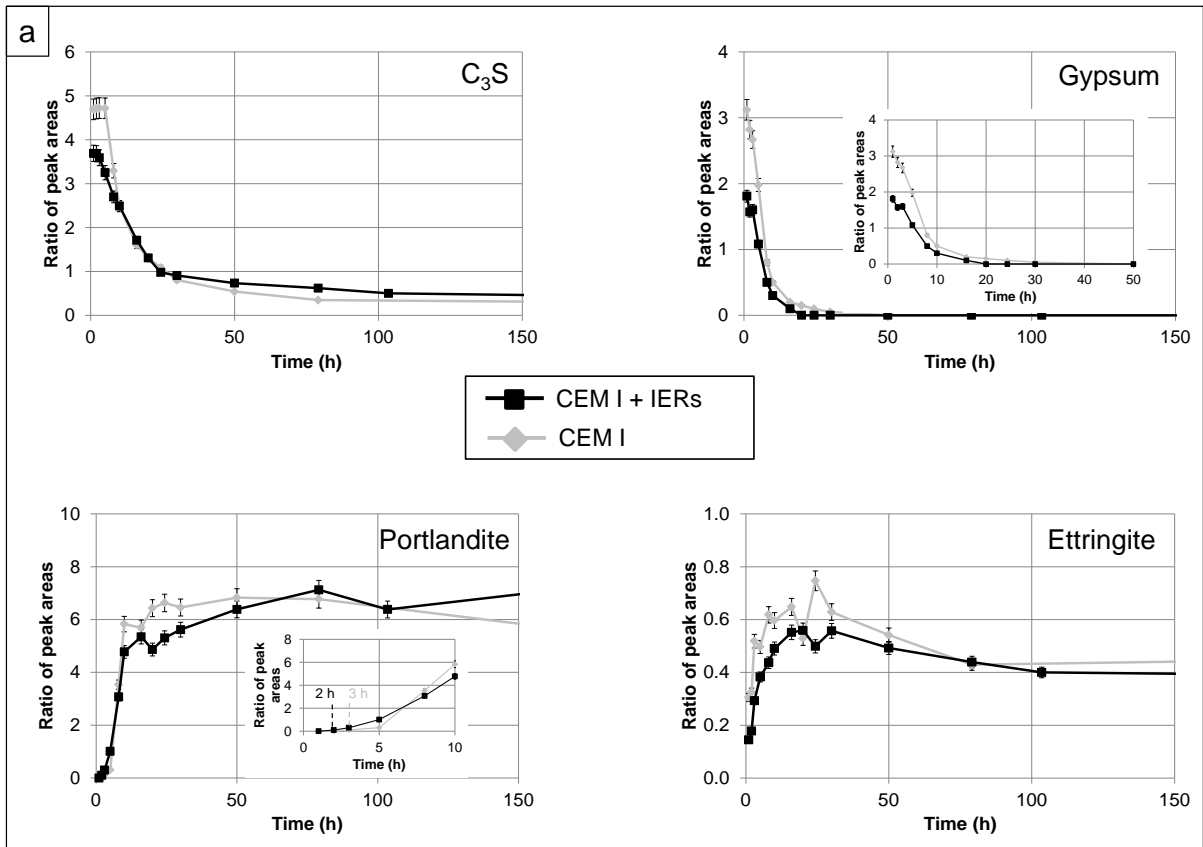
Figure 7: X-ray diffraction patterns of IERs-CEM III/C samples.



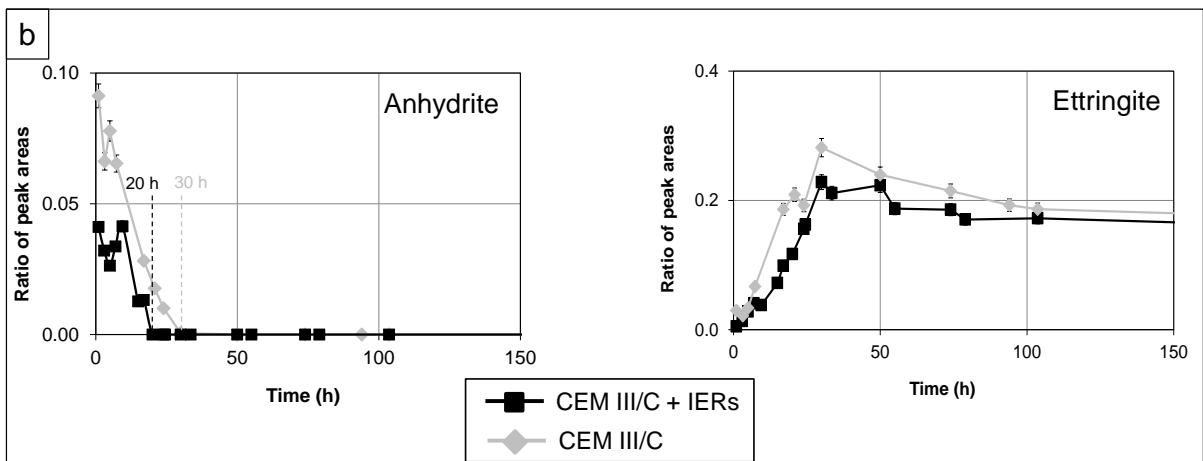
355

356

357 Figure 8: Influence of the resins on the phase content of CEM I (a) and CEM III/C (b) cement pastes  
 358 during hydration.



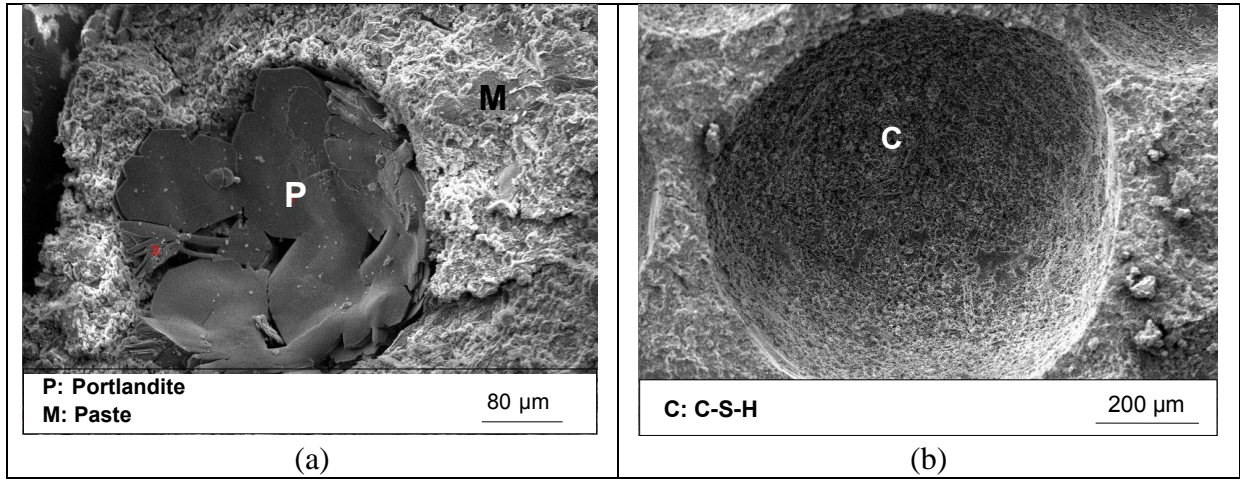
359



360

361

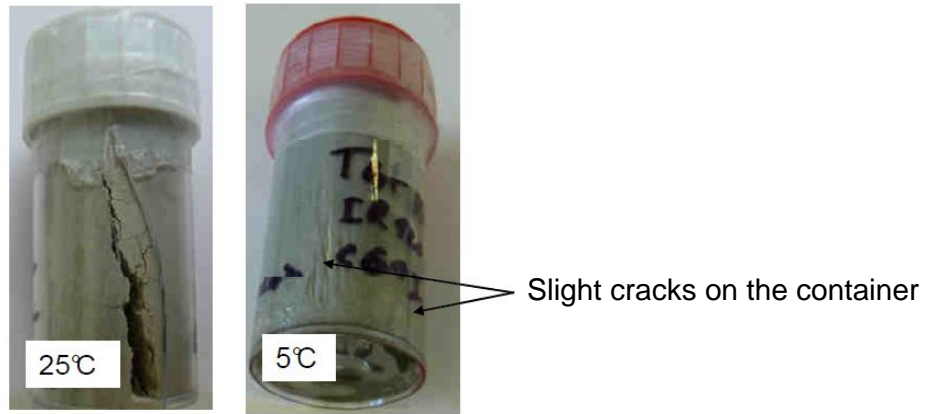
362 Figure 9: SEM observation of IERs-cement forms aged of 2 months: cavity previously occupied by a  
363 resin bead. (a) CEM I sample; (b) CEM III/C sample.



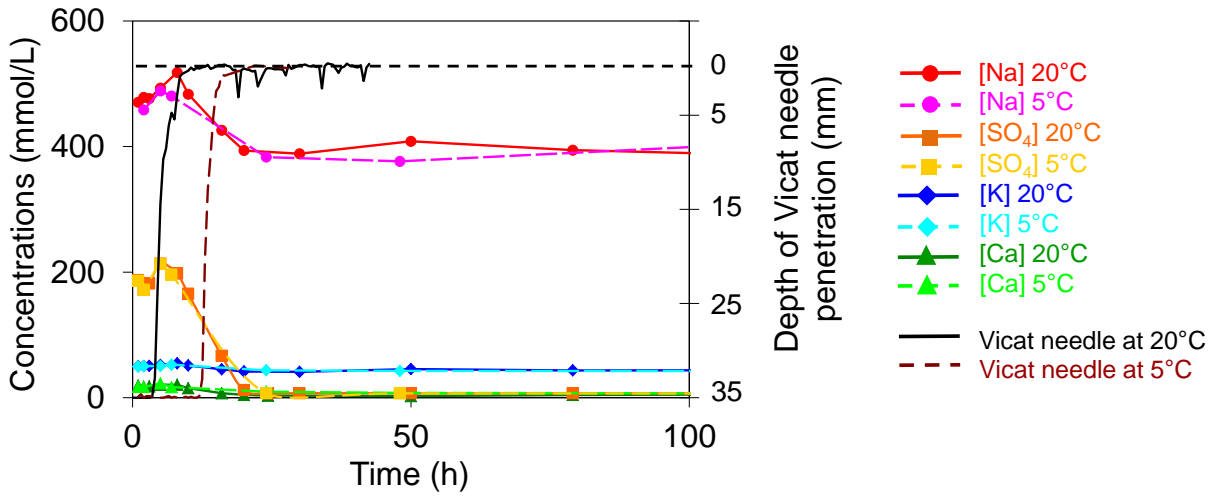
364

365

366 Figure 10: IERs-CEM I samples cured for 6 days at 25°C (left) or 5°C (right).



370 Figure 11 : Evolution of the interstitial solution composition ( $\text{Na}^+$ ,  $\text{K}^+$ ,  $\text{Ca}^{2+}$ ,  $\text{SO}_4^{2-}$ ) and Vicat needle  
 371 penetration versus time for IERs-CEM I samples cured at 5 and 20 °C..



372